ANTIOXIDANTS & REDOX SIGNALING
Volume 26, Number 14, 2017

DOI: 10.1089/ars.2015.6571

FORUM ORIGINAL RESEARCH COMMUNICATION

Control of Oxidative Stress and Inflammation in Sickle Cell Disease with the Nrf2 Activator Dimethyl Fumarate

John D. Belcher,[1] Chunsheng Chen,[1] Julia Nguyen,[1] Ping Zhang,[1] Fuad Abdulla,[1] Phong Nguyen,[1] Trevor Killeen,[1] Pauline Xu,[1] Gerry O'Sullivan,[2] Karl A. Nath,[3] and Gregory M. Vercellotti[1]

Abstract

Aims: Heme derived from hemolysis is pro-oxidative and proinflammatory and promotes vaso-occlusion in murine models of sickle cell disease (SCD), suggesting that enhanced detoxification of heme may be beneficial. Nuclear factor erythroid-2-related factor-2 (Nrf2) transcription pathway is the principal cellular defense system responding to pro-oxidative and proinflammatory stress. Dimethyl fumarate (DMF), a drug approved for treatment of multiple sclerosis, provides neuroprotection by activating Nrf2-responsive genes. We hypothesized that induction of Nrf2 with DMF would be beneficial in murine SCD models.
Results: DMF (30 mg/kg/day) or vehicle (0.08% methyl cellulose) was administered for 3–7 days to NY1DD and HbSS-Townes SCD mice. Vaso-occlusion, a hallmark of SCD, measured in sickle mice with dorsal skinfold chambers, was inhibited by DMF. The inhibitory effect of DMF was abrogated by the heme oxygenase-1 (HO-1) inhibitor tin protoporphyrin. DMF increased nuclear Nrf2 and cellular mRNA of Nrf2-responsive genes in livers and kidneys. DMF increased heme defenses, including HO-1, haptoglobin, hemopexin, and ferritin heavy chain, although plasma hemoglobin and heme levels were unchanged. DMF decreased markers of inflammation, including nuclear factor-kappa B phospho-p65, adhesion molecules, and toll-like receptor 4. DMF administered for 24 weeks to HbSS-Townes mice decreased hepatic necrosis, inflammatory cytokines, and irregularly shaped erythrocytes and increased hemoglobin F, but did not alter hematocrits, reticulocyte counts, lactate dehydrogenase, plasma heme, or spleen weights, indicating that the beneficial effects of DMF were not attributable to decreased hemolysis.
Innovation: These studies identify Nrf2 activation as a new therapeutic target for the treatment of SCD.
Conclusion: DMF activates Nrf2, enhances antioxidant defenses, and inhibits inflammation and vaso-occlusion in SCD mice. *Antioxid. Redox Signal.* 26, 748–762.

Keywords: Nrf2, HO-1, sickle cell disease, haptoglobin, hemopexin

Introduction

PATIENTS WITH SICKLE CELL DISEASE (SCD) have unrelenting hemolysis that continually releases hemoglobin and heme into the vasculature. Heme, a damage-associated molecular pattern, can activate the pattern recognition receptor toll-like receptor 4 (TLR4), leading to oxidative stress, inflammation, and vaso-occlusion (5, 13, 22). Intravenous infusion of the hemoglobin-binding protein haptoglobin or the heme-binding protein hemopexin into sickle mice inhibits

Innovation

Only one drug, hydroxyurea, has been approved for the treatment of sickle cell disease (SCD). These studies identify nuclear factor erythroid-2-related factor-2 (Nrf2) activation as a new therapeutic target for the treatment of SCD. These findings help provide impetus for clinical testing of dimethyl fumarate in SCD patients.

[1]Division of Hematology, Oncology and Transplantation, Department of Medicine, Vascular Biology Center, University of Minnesota, Minneapolis, Minnesota.
[2]Veterinary Population Medicine, University of Minnesota, St. Paul, Minnesota.
[3]Division of Nephrology and Hypertension, Department of Medicine, Mayo Clinic/Foundation, Rochester, Minnesota.

vaso-occlusion in the steady state or after hemoglobin challenge (5). Moreover, induction of the cytoprotective heme metabolizing enzyme heme oxygenase-1 (HO-1) or the iron-binding protein ferritin heavy chain (FHC) induces cellular cytoprotective responses that inhibit oxidative stress, inflammation, and vaso-occlusion in humanized SCD mice (6, 9, 58).

The master regulator of cellular cytoprotective responses to heme, iron, and oxidative stress is nuclear factor erythroid-2-related factor-2 (Nrf2) (51). Nrf2 activity is controlled, in part, by the cytosolic protein, kelch-like ECH-associated protein 1 (Keap1) (44). Nrf2 is located in the cytoplasm when bound to Keap1. The Nrf2/Keap1 complex turns over rapidly *via* ubiquitination and proteasomal degradation. Reactive sulfhydryls on Keap1 can be readily oxidized by reactive oxygen species and electrophiles, thereby releasing Nrf2, allowing it to translocate to the nucleus where it activates target genes that possess antioxidant response elements (ARE) in their promoter regions. Studies comparing basal and stress-induced responses in various tissues of wild-type and Nrf2-deficient mice have identified a large number of cytoprotective genes that are transcribed in response to Nrf2 activation (14, 27, 50, 55, 62).

Dimethyl fumarate (DMF) induces endogenous antioxidant defenses in neuronal cells and astrocytes *via* the Nrf2 pathway (1, 15, 35, 36, 42, 63). DMF and its primary metabolite, monomethyl fumarate (MMF), alkylate a critical reactive thiol, Cys151, on Keap1 causing release of Nrf2, nuclear localization, and activation of cellular anti-inflammatory responses (36, 48). In patients with relapsing-remitting multiple sclerosis, DMF significantly reduced the proportion of patients with relapse, the relapse rate, disability progression, and the number of lesions (23). The Food and Drug Administration in the United States and their European, Canadian, and Australian counterparts approved enteric coated DMF (Tecfidera) for the treatment of multiple sclerosis. Based on these studies and the anti-inflammatory properties of DMF, we examined the cytoprotective effects of DMF in humanized mouse models of SCD. These studies further our observations of protection afforded by DMF in sickle mice that were initially reported as an oral abstract at the American Society of Hematology in December 2014 (8).

Results

Vaso-occlusion is a hallmark of SCD. Heme-induced vaso-occlusion (stasis) was measured in the subcutaneous venules of NY1DD and HbSS-Townes sickle mice with implanted dorsal skinfold chambers (DSFCs). These two murine models of SCD were chosen because of their robust inflammation and vaso-occlusion and their differential expression of human γ-globin. HbSS-Townes mice are genetically capable of expressing human $^{A}\gamma$-globin and thus the γ-globin-containing hemoglobin F (HbF). In contrast, the NY1DD mice do not harbor the human γ-globin gene and do not express HbF. Thus, these two models allowed us to examine the effects of DMF independently of the human γ-globin gene, which can inhibit hemolysis (53) and which is upregulated by the DMF metabolite MMF in human erythroid cells (46). In NY1DD mice administered vehicle, microvascular stasis was 29% and 24% at 1 and 4 h, respectively, after heme infusion (Fig. 1A). In contrast, in NY1DD mice administered DMF, stasis was reduced to 6% and 4% at 1 and 4 h, respectively, after heme infusion ($p < 0.001$ compared to vehicle). The inhibitory effects of DMF on vaso-occlusion were abrogated in NY1DD mice administered the HO-1 inhibitor tin protoporphyrin (SnPP). This observation on the importance of HO-1 activity for inhibiting heme-induced vaso-occlusion in SCD also has been made with vaso-occlusion induced by hypoxia–reoxygenation (6, 10). In HbSS-Townes mice administered vehicle, microvascular stasis was 33% and 31% at 1 and 4 h, respectively, after heme infusion (Fig. 1B). In contrast, in HbSS-Townes mice administered DMF, stasis was reduced to 9% and 6% at 1 and 4 h, respectively, after heme infusion ($p < 0.001$).

Relative nuclear Nrf2 expression was determined by Western blots of nuclear extracts isolated from the livers and kidneys of sickle mice treated with DMF or vehicle. In NY1DD mice (Fig. 2A), DMF administration increased nuclear Nrf2 expression 5.6-fold ($p = 0.029$) in livers and 2.5-fold ($p < 0.01$) in kidneys compared to vehicle-treated mice. Similarly, in HbSS-Townes mice (Fig. 2B), DMF increased nuclear Nrf2 expression 3.5-fold ($p < 0.001$) in livers and 3.9-fold ($p < 0.001$) in kidneys.

We examined mRNA levels of several previously reported Nrf2-responsive genes in the livers and kidneys of sickle mice administered DMF or vehicle. The relative mRNA levels of HO-1, FHC, haptoglobin, hemopexin, Nrf2, ferroportin, glutamate–cysteine ligase catalytic subunit, glutathione S-transferase alpha-2 (GSTA2), NAD(P)H dehydrogenase [quinone]-1, glutathione S-transferase mu-1, and multidrug resistance-associated protein-2 were enriched 1.7–4.4-fold in the livers and 0.3–3.4-fold in the kidneys of DMF-treated NY1DD mice (Table 1) and 1.9–3.5-fold in the livers and 0.14–20.5-fold in the kidneys of HbSS-Townes mice (Table 2). DMF administration significantly increased mRNA levels for all of the Nrf2-responsive genes evaluated in the livers of NY1DD and HbSS-Townes mice, but not in the kidneys. Glutathione S-transferases function in the detoxification of electrophilic compounds and products of oxidative stress by conjugation with glutathione. The GSTA class is the most abundantly expressed glutathione S-transferases in the liver. In addition to metabolizing bilirubin, GSTA exhibits glutathione peroxidase activity, thereby protecting the cells from reactive oxygen species and the products of peroxidation. We examined protein expression for GSTA2 in the cytosol of livers from HbSS-Townes mice. Cytosolic GSTA2 expression increased 4.8-fold ($p < 0.01$) in the livers of mice administered DMF relative to vehicle (Supplementary Fig. S1; Supplementary Data are available online at www.liebertpub.com/ars).

HO-1 is a master anti-inflammatory gene and its expression is controlled in part by Nrf2. HO-1 expression is increased in tissues of SCD mice and patients (6, 28, 33, 43). Additional induction of HO-1 activity in SCD mice significantly inhibits markers of tissue inflammation and vaso-occlusion (6, 9). In NY1DD mice, oral DMF administration increased HO-1 expression 9.6-fold ($p < 0.001$) in livers (Fig. 3A) and 10.7-fold ($p < 0.001$) in kidneys (Fig. 3B) compared to vehicle-treated mice. Similarly, in HbSS-Townes mice, DMF increased HO-1 expression 4.0-fold ($p < 0.01$) in livers (Fig. 3C) and 4.6-fold ($p < 0.05$) in kidneys (Fig. 3D). Hepatic HO-1 activity was increased three to fivefold in DMF-treated sickle mice relative to vehicle-treated mice (data not shown).

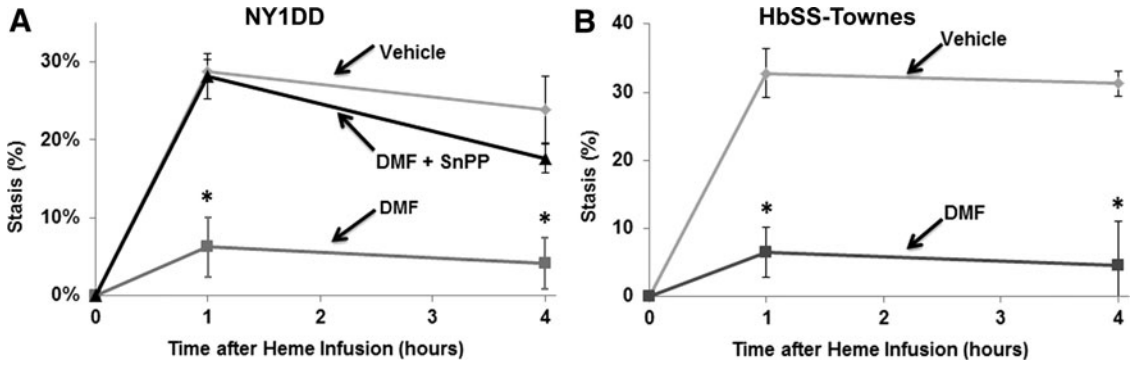

FIG. 1. DMF inhibits heme-induced vaso-occlusion (stasis) in sickle mice. (A) NY1DD ($n=4$/group) and **(B)** HbSS-Townes ($n=3$/group) sickle mice with implanted dorsal DSFCs were administered DMF (30 mg/kg) or vehicle for 3 or 7 days, respectively. At baseline, on the last day of treatment, 20–30 flowing venules were selected and mapped using intravital microscopy. After venule selection and mapping, heme (3.2 μmol/kg) was infused into the tail vein. At 1 and 4 h after heme infusion, the same venules were re-examined to determine if they were flowing or not flowing (stasis). The percent stasis was calculated at each time point. In one cohort of NY1DD mice ($n=4$) in **(A)**, the HO-1 inhibitor, SnPP was administered (40 μmol/kg, i.p.) for 3 consecutive days before stasis measurement. Values are mean ± SD. *$p<0.001$ for DMF *versus* vehicle. DMF, dimethyl fumarate; DSFC, dorsal skinfold chamber; HO-1, heme oxygenase-1; SnPP, tin protoporphyrin.

Iron, released from heme by HO-1, is ultimately placed as ferric iron (Fe^{3+}) in the core of ferritin. We previously demonstrated that *Sleeping Beauty*-mediated overexpression of FHC in humanized SCD mice inhibits inflammation and vaso-occlusion independently of HO-1 activity (58). In NY1DD mice, DMF administration increased FHC expression 2.7-fold ($p<0.001$) in livers (Fig. 4A) and 2.6-fold ($p=0.003$) in kidneys (Fig. 4B) compared to vehicle-treated mice. In HbSS-Townes mice, DMF increased FHC expression 10.2-fold ($p<0.001$) in livers (Fig. 4C) and 2.6-fold ($p<0.001$) in kidneys (Fig. 4D).

Plasma haptoglobin and hemopexin are depleted in SCD mice and patients (41, 60). Infusion of purified haptoglobin or hemopexin into SCD mice inhibits vaso-occlusion in unchallenged SCD mice in the steady state and in SCD mice in response to a hemoglobin challenge (5). We examined relative plasma haptoglobin and hemopexin levels in DMF- and vehicle-treated mice. In NY1DD mice (Fig. 5A), DMF administration increased plasma haptoglobin expression 2.1-fold ($p=0.023$) and plasma hemopexin expression 3.5-fold ($p=0.002$) compared to vehicle-treated mice. The induction of haptoglobin and hemopexin was even greater in the plasma

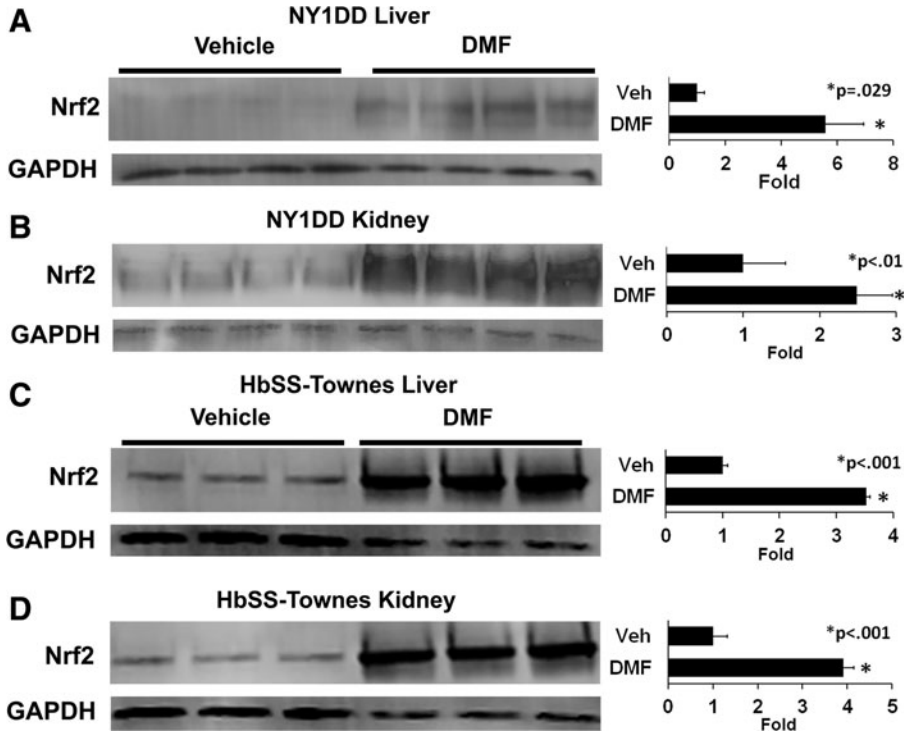

FIG. 2. DMF increases nuclear Nrf2 expression in livers and kidneys of sickle mice. (A, B) NY1DD ($n=4$/group) and **(C, D)** HbSS-Townes ($n=3$/group) sickle mice with implanted DSFCs were administered DMF (30 mg/kg) or vehicle for 3 or 7 days, respectively. The mice were sacrificed, and the livers and kidneys were removed and frozen 4 h after the infusion of heme and the measurement of stasis. Liver and kidney nuclear extracts were isolated, run on Western blots, and immunostained for Nrf2 (98 kDa) and GAPDH (36 kDa). Nrf2, nuclear factor erythroid-2-related factor-2.

Table 1. NY1DD Mice: Enrichment of Gene-Specific mRNA in Livers and Kidneys of Dimethyl Fumarate-Treated Mice

	Livers		*Kidneys*	
mRNA	*Fold enrichment*	p-*Value*	*Fold enrichment*	p-*Value*
HO-1	1.7	0.020	2.5	0.022
FHC	2.6	0.001	2.1	0.001
Haptoglobin	2.7	0.046	0.6	0.460
Hemopexin	2.5	0.023	0.3	0.020
Nrf2	2.7	0.004	1.7	0.043
Ferroportin	3.1	0.001	2.1	0.007
Glutamate–cysteine ligase catalytic subunit	3.3	0.001	1.8	0.009
GSTA2	3.4	0.032	2.1	0.222
NAD(P)H dehydrogenase [quinone]-1	3.8	0.008	3.4	0.023
Glutathione S-transferase Mu 1	3.8	0.001	2.9	0.002
Multidrug resistance-associated protein 2	4.4	0.001	1.9	0.001

Fold enrichment values are calculated as gene-specific mRNA to GAPDH ratios in DMF-treated organs divided by gene-specific mRNA to GAPDH ratios in vehicle-treated organs. NY1DD ($n=4$/group) sickle mice with implanted DSFCs were administered DMF (30 mg/kg) or vehicle for 3 days.

DMF, dimethyl fumarate; DSFC, dorsal skinfold chamber; FHC, ferritin heavy chain; GSTA2, glutathione S-transferase alpha 2; HO-1, heme oxygenase-1; Nrf2, nuclear factor erythroid-2-related factor-2.

of HbSS-Townes mice (Fig. 5B), DMF increased plasma haptoglobin expression 6.9-fold ($p<0.01$) and plasma hemopexin expression 3.5-fold ($p=0.002$). Despite increased plasma haptoglobin and hemopexin expression in DMF-treated mice, mean total plasma heme (Fig. 5C) concentrations were not significantly different between treatment groups in NY1DD and HbSS-Townes mice.

Since free heme can activate TLR4 signaling in tissues leading to nuclear factor-kappa B (NF-κB) activation, inflammatory responses, and vaso-occlusion (5), we examined the effects of DMF administration on TLR4 expression and markers of inflammation. In NY1DD mice, DMF administration inhibited hepatic TLR4 expression 2.9-fold ($p=0.001$) compared to vehicle-treated mice (Fig. 6A). DMF administration also inhibited hepatic NF-κB activation relative to vehicle-treated mice as indicated by a decrease in nuclear phospho-p65 expression 3.2-fold ($p<0.001$) compared to vehicle-treated mice (Fig. 6B). Total nuclear p65 was similar in both treatment groups. In concordance with inhibition of NF-κB activation, adhesion molecules vascular cell adhesion molecule-1 (VCAM-1), intercellular adhesion molecule-1 (ICAM-1), and E-selectin were decreased 2.5–4.1-fold in the livers of DMF-treated NY1DD mice (Fig. 6C).

Hepatic necrosis is a prominent pathologic feature in mouse models of SCD. We administered DMF ($\sim$30 mg/kg/day) or vehicle in the drinking water of HbSS-Townes mice for 24 weeks and examined the effects of DMF on liver necrosis (Fig. 7). Necrotic areas were delineated and their areas measured. Examples of acute and chronic necrotic lesions in vehicle- and DMF-treated mice are presented in Figure 7A and B. Areas of these acute and chronic lesions in livers were measured and expressed as a percentage of the total measured areas. Sickle mice administered DMF had a mean necrotic area of 0.9% compared to 2.1% in livers from vehicle-treated

Table 2. HbSS-Townes Mice: Enrichment of Gene-Specific mRNA in Livers and Kidneys of Dimethyl Fumarate-Treated Mice

	Livers		*Kidneys*	
mRNA	*Fold enrichment*	p-*Value*	*Fold enrichment*	p-*Value*
HO-1	2.6	0.042	1.7	0.070
FHC	3.5	0.004	1.8	0.030
Haptoglobin	1.9	0.045	0.14	0.180
Hemopexin	2.4	0.022	0.42	0.138
Nrf2	2.3	0.018	1.5	0.014
Ferroportin	2.7	0.008	2.0	0.065
Glutamate–cysteine ligase catalytic subunit	2.6	0.016	1.9	0.034
GSTA2	2.9	0.042	20.5	0.046
NAD(P)H dehydrogenase [quinone]-1	2.9	0.026	2.8	0.021
Glutathione S-transferase Mu 1	3.0	0.009	2.1	0.006
Multidrug resistance-associated protein 2	2.4	0.030	3.6	0.024

Fold enrichment values are calculated as gene-specific mRNA to GAPDH ratios in DMF-treated organs divided by gene-specific mRNA to GAPDH ratios in vehicle-treated organs. HbSS-Townes ($n=3$/group) sickle mice with implanted DSFCs were administered DMF ($\sim$30 mg/kg) or vehicle for 7 days.

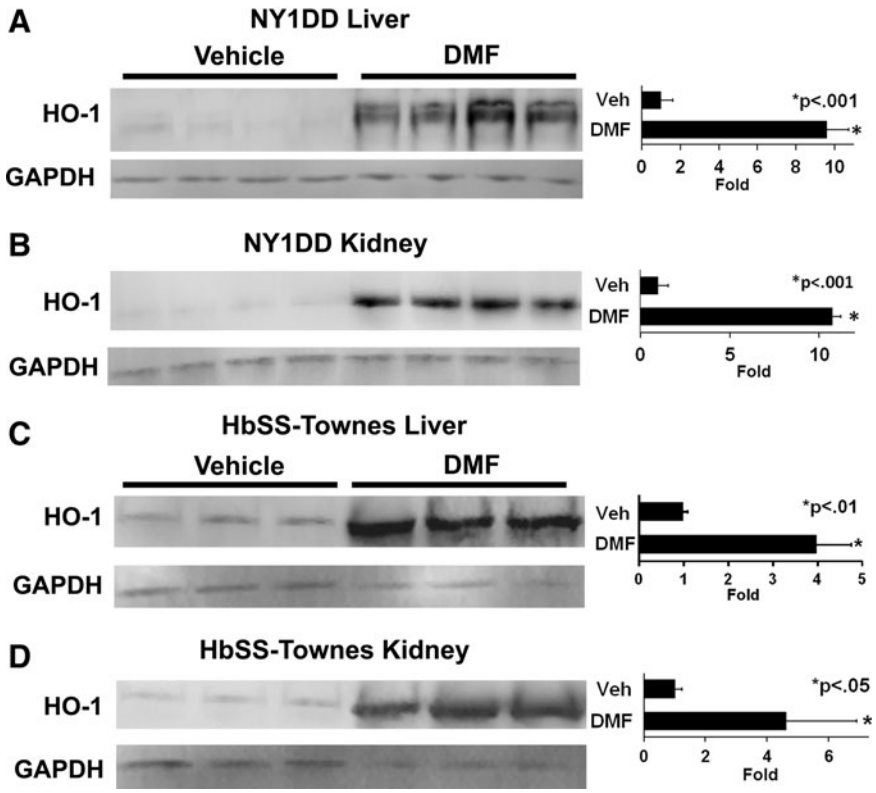

FIG. 3. DMF increases HO-1 expression in livers and kidneys of sickle mice. (A, B) NY1DD ($n=4$/group) and **(C, D)** HbSS-Townes ($n=3$/group) sickle mice with implanted DSFCs were administered DMF (30 mg/kg) or vehicle for 3 or 7 days, respectively. The mice were sacrificed, and the livers and kidneys were removed and frozen 4 h after the infusion of heme and the measurement of stasis. Liver and kidney microsomes were isolated, run on Western blots, and immunostained for HO-1 (32 kDa) and GAPDH (36 kDa).

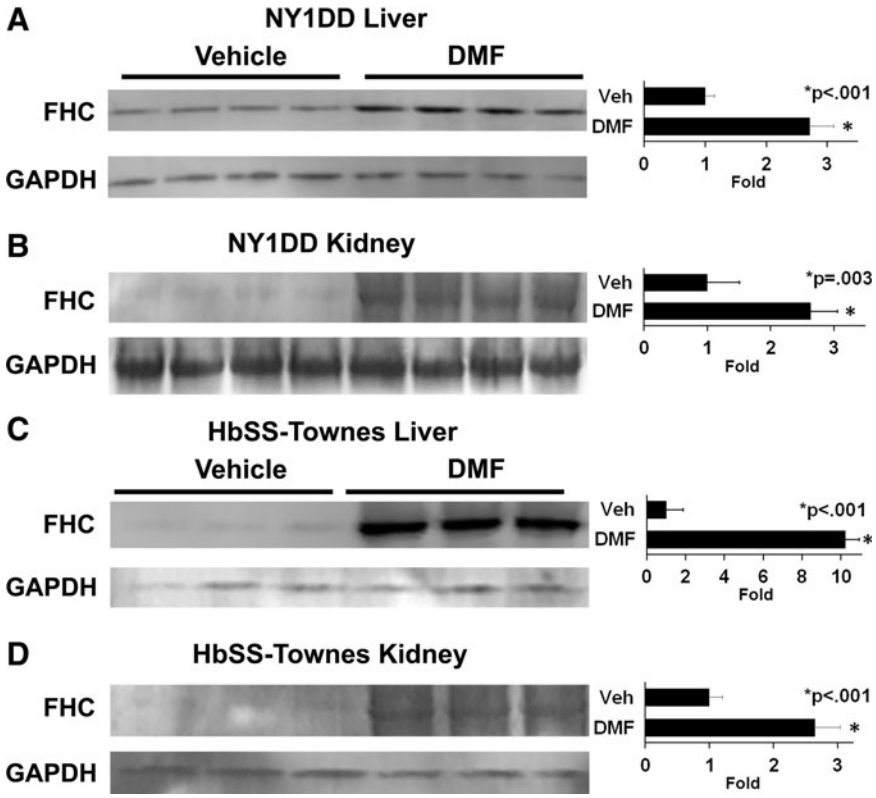

FIG. 4. DMF increases FHC in livers and kidneys of sickle mice. (A, B) NY1DD ($n=4$/group) and **(C, D)** HbSS-Townes ($n=3$/group) sickle mice with implanted DSFCs were administered DMF (30 mg/kg) or vehicle for 3 or 7 days, respectively. The mice were sacrificed, and the livers and kidneys were removed and frozen 4 h after the infusion of heme and the measurement of stasis. Liver and kidney microsomes were isolated, run on Western blots, and immunostained for FHC (21 kDa) and GAPDH (36 kDa). FHC, ferritin heavy chain.

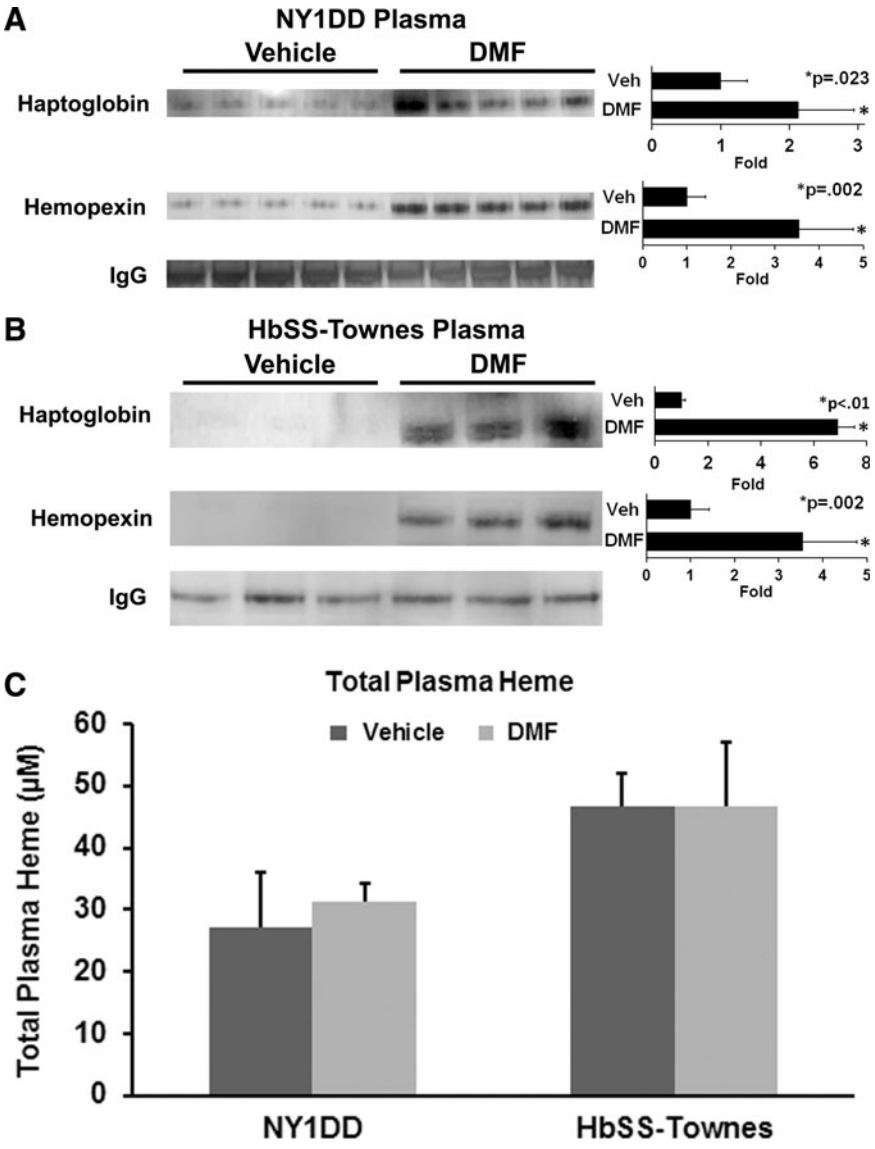

FIG. 5. DMF increases plasma haptoglobin and hemopexin levels sickle mice. Plasma was collected from the abdominal aortas of anesthetized sickle mice without implanted DSFCs and heme infusion before collection. **(A)** NY1DD ($n=5$/group) and **(B)** HbSS-Townes ($n=3$/group) sickle mice were administered DMF or vehicle for 7 days. Plasma was run on Western blots and immunostained for haptoglobin (45 kDa), hemopexin (68 kDa), or IgG (155 kDa). **(C)** Total plasma heme levels were also measured in NY1DD and HbSS-Townes mice after 2 or 24 weeks of treatment, respectively.

mice (Fig. 7C, $p=0.039$). DMF administration to HbSS-Townes mice also decreased hepatic mRNA of proinflammatory cytokines IL-6, IL-1β, and IL-18 to 17%, 45%, and 27% of vehicle-treated mice, respectively (Fig. 7D). Cytoplasm contains a number of antioxidant enzymes. Mean cytoplasmic levels of protein carbonyls, a marker of protein oxidation, were 33% lower in DMF-treated HbSS-Townes mice than vehicle-treated sickle mice ($p<0.05$, Supplementary Fig. S2). Despite significant decreases in hepatic necrotic areas, inflammatory cytokine mRNA, and protein carbonyls, there was no significant difference in plasma aspartate aminotransferase (AST), a marker of organ dysfunction, between DMF- and vehicle-treated mice (data not shown). In other data not shown, hepatic 4-hydroxynonenal (4-HNE), a marker of lipid peroxidation, and 24-h urinary 8-hydroxydeoxyguanosine, a marker of DNA oxidation, were both 30% lower in DMF-treated mice compared to vehicle, but the differences were not significant ($p=0.30$ and $p=0.12$, respectively). In addition, urinary creatinine was 27% lower in DMF-treated mice compared to vehicle ($p=0.167$).

Hematologic parameters were measured in HbSS-Townes mice after 1 and 24 weeks of treatment with vehicle or DMF. MMF, the primary metabolite of DMF, induces γ-globin expression and HbF production in cultured human erythroid cells (46). At high enough concentrations, HbF can inhibit hemoglobin S (HbS) polymerization and subsequent hemolysis (53). HbSS-Townes mice have the human α and $^{A}\gamma\beta^{S}$ globin genes and thus are genetically capable of expressing human $^{A}\gamma$-globin and HbF. Oral administration of DMF to HbSS-Townes mice for 24 weeks increased the percentage of HbF-containing red blood cells (F-cells) to 8.8% compared to 4.2% in vehicle-treated mice ($p=0.043$; Table 3). The red blood cells (RBC) displayed a wide variation in shapes (*poikilocytosis*). The irregular shaped RBC, counted and expressed as a percentage of total RBC, were markedly elevated in HbSS-Townes mice. These irregular shapes included teardrop > schistocyte > elliptocyte > bite > and sickle (37). These irregular shaped RBC decreased from 25.3% in vehicle-treated mice to 19.0% in DMF-treated mice ($p<0.05$). Despite the modest increase in F-cells and decrease in

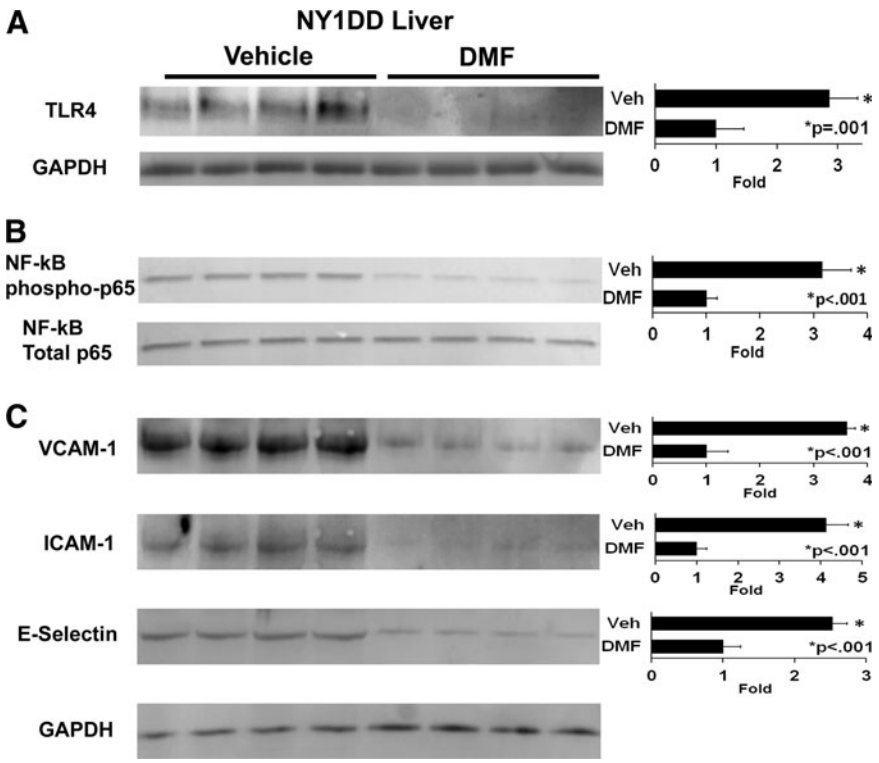

FIG. 6. DMF decreases markers of inflammation in livers of NY1DD mice. NY1DD ($n=4$/group) sickle mice with implanted DSFCs were administered DMF (30 mg/kg) or vehicle for 3 days. The mice were sacrificed, and the livers were removed and frozen 4 h after the infusion of heme and the measurement of stasis. Liver subfractions were isolated, run on Western blots, and immunostained for **(A)** microsomal TLR4 (95 kDa) and GAPDH (36 kDa), **(B)** nuclear phospho- and total p65 NF-kB (65 kDa), and **(C)** microsomal VCAM-1 (100 kDa), ICAM-1 (99 kDa), and E-selectin (67 kDa). ICAM-1, intercellular adhesion molecule-1; NF-κB, nuclear factor-kappa B; TLR4, toll-like receptor 4; VCAM-1, vascular cell adhesion molecule-1.

irregular shaped RBC, markers of hemolysis, including hematocrit, percent reticulocytes, total plasma heme, plasma lactate dehydrogenase (LDH), and spleen weight as a percent of body weight (Table 3), were not significantly different between DMF- and vehicle-treated HbSS-Townes mice after 1 or 24 weeks of treatment. Interestingly, there was an age-related decline in hematocrits and an increase in reticulocytes in both vehicle- and DMF-treated HbSS-Townes mice when comparing mice 10 weeks of age to mice 28 weeks of age, suggesting an age-related increase in RBC destruction ($p<0.05$ for both treatment groups, Table 3). White blood cell counts were markedly elevated, but not significantly different between DMF- and vehicle-treated HbSS-Townes mice. No differences were seen in plasma AST levels between DMF- and vehicle-treated mice (data not shown).

Discussion

DMF is an electrophilic thioreactive alkene (16, 24) that is protective against electrophile toxicity and oxidative stress (52). These studies demonstrate that the administration of DMF to humanized mouse models of SCD inhibits heme-induced vaso-occlusion in an HO-1-dependent manner, activates nuclear Nrf2 expression, and increases the transcription and expression of Nrf2-responsive genes, including proteins involved in hemoglobin, heme, and iron clearance, decreases markers of inflammation, including TLR4, NF-κB activation, adhesion molecule expression, and proinflammatory cytokines, decreases necrotic lesions in livers, and increases circulating F-cells without decreasing hemolysis.

The vasculature of SCD patients is bathed in heme for a lifetime. Free heme promotes an activated proinflammatory, proadhesive, and prothrombotic phenotype. Previous studies demonstrated that enhancing the degradation of heme by increasing HO-1 activity was beneficial in murine models of SCD (6, 9). HO-1 gene therapy targeted to the liver in SCD mice inhibited vascular inflammation and vaso-occlusion in a distally implanted DSFC (9). HO-1 polymorphism studies in SCD children also supported a beneficial role for HO-1 (4). A (GT)(n) dinucleotide repeat located in the promoter region of the human HO-1 gene is highly polymorphic, with short repeat lengths linked to increased HO-1 expression and a decreased risk of acute chest syndrome in children with SCD. DMF is a potent inducer of the Nrf2/HO-1 axis (20), and therefore, a logical drug candidate for the treatment of SCD. The protection against vaso-occlusion afforded by DMF appeared to be dependent on HO-1 activity, as SnPP, a potent inhibitor of HO-1 activity, reversed the anti-vaso-occlusive properties of DMF administration. Additional studies in HO-1-deficient sickle mice are needed to confirm this observation.

DMF and its primary intestinal metabolite MMF can react with cysteine-151 on Keap1/Nrf2 complexes in the cytoplasm (Fig. 8) (54). The most probable reaction is a Michael addition of the nucleophilic sulfhydryl on Cys151 to the electrophilic alkene bond of MMF (21). Alkylation of the Keap1 sulfhydryl allows dissociation and stabilization of Nrf2, allowing Nrf2 to accumulate in the nucleus where it can bind to AREs located in the regulatory regions of a battery of cellular defense genes and thereby activate transcription of those genes (64). HO-1, FHC, haptoglobin, hemopexin, and multiple other antioxidant genes have been previously identified as Nrf2-responsive genes in studies comparing gene expression in wild-type and Nrf2 null mice with and without Nrf2 agonists (12, 14, 27, 50, 57, 62).

Extracellular hemoglobin in hemolytic patients is associated with adverse clinical outcomes, such as vascular

disease, inflammation, thrombosis, and renal injury. Extracellular hemoglobin can be transported into the extravascular space, catalyze pro-oxidative and hypertensive reactions, and release heme. Sequestration of extracellular hemoglobin with haptoglobin in animal models prevents hemoglobin-induced hypertension, oxidant damage to the kidney, and markedly inhibits vaso-occlusion in SCD mice (11, 30, 49). However, haptoglobin levels are depleted in SCD (41, 60); interventions to increase plasma haptoglobin levels in SCD patients may be beneficial by preventing oxidative reactions with hemoglobin and the release of free heme into the vasculature (5, 39, 49).

Plasma hemopexin is capable of abrogating all of the pro-oxidative, proinflammatory, and procoagulant effects of cell-free heme (2, 3, 5, 22, 25, 34, 56, 60). Hemopexin is produced in the liver and circulates in plasma. Hemopexin has the highest affinity for heme ($K_d < 10^{-13}$) of any known protein and can remove heme from lower affinity plasma proteins like albumin (40). Unlike albumin–heme complexes, hemopexin–heme complexes do not activate proinflammatory TLR4 signaling (5) and are safely removed from the plasma by low-density lipoprotein receptor-related protein 1 (LRP1/CD91) receptors on hepatocytes and macrophages (26). However, like haptoglobin, plasma hemopexin levels are depleted in SCD patients and mice (41, 60). Hemopexin supplementation in SCD mice prevents heme-induced endothelial toxicity (60). Like haptoglobin, therapies such as DMF that increase plasma hemopexin levels may be beneficial in SCD patients and other hemolytic conditions by delivering heme safely to the liver and subsequently inducing hepatic Nrf2 and HO-1 (59). The lack of induction of haptoglobin and hemopexin mRNA in the kidneys (Tables 1 and 2) probably reflects the dominant role of the liver in their synthesis.

Why did increased plasma haptoglobin and hemopexin levels not result in decreased plasma heme? The method used to measure plasma heme levels measures total plasma heme, including heme bound to microparticles, hemoglobin, albumin, haptoglobin, and hemopexin (unpublished data). We also measured the heme concentration in protein-depleted plasma (MW <3 kDa) from mice treated with vehicle and DMF. The mean ± SD plasma protein-free heme concentrations were $2.48 \pm 1.45\ \mu M$ in vehicle-treated mice and $2.77 \pm 1.01\ \mu M$ in DMF-treated mice. The mean difference was not significantly different. The low levels of protein-depleted heme in plasma are not surprising because free heme is relatively insoluble in water or physiological solutions (19). Plasma hemoglobin and heme levels reflect only a snapshot in time and do not reflect the rapid throughput of heme from the RBC to the tissues, which occurs continuously in SCD. These data shed no light on the production and clearance rates of plasma hemoglobin,

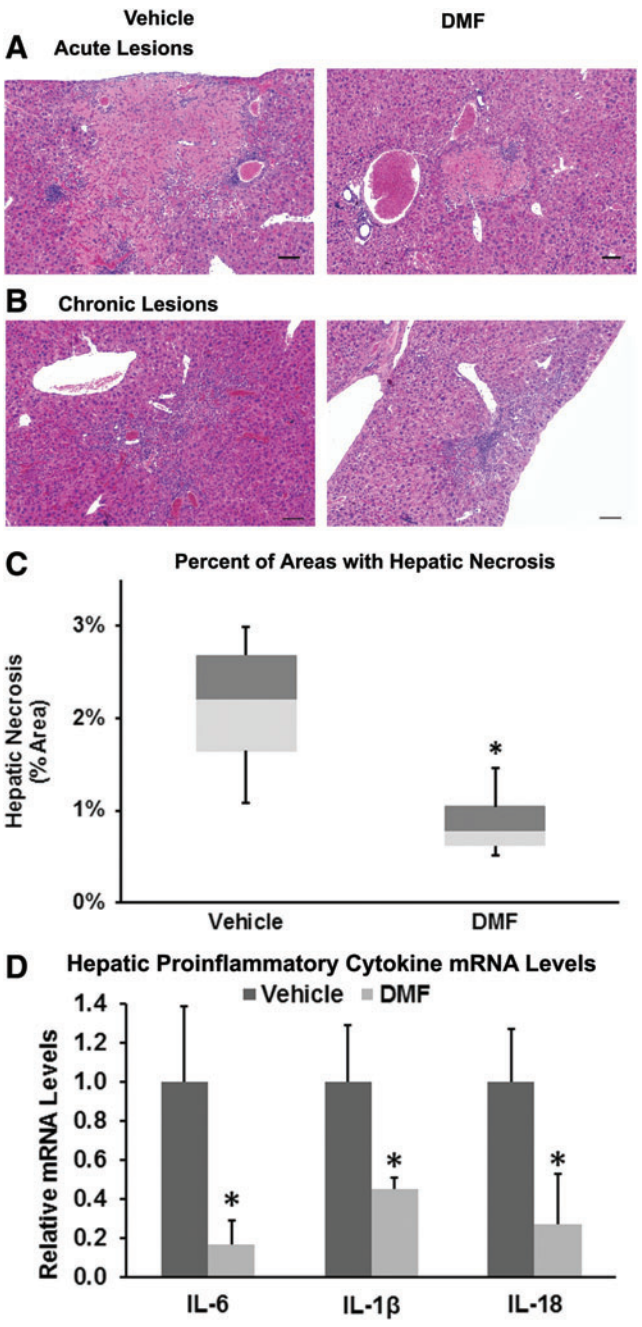

FIG. 7. Chronic DMF administration decreases hepatic necrosis in livers of sickle mice. HbSS-Townes ($n = 4$/group) sickle mice were treated with oral DMF (~30 mg/kg/day) or vehicle in drinking water for 24 weeks, beginning at 4 weeks of age. Liver sections were stained with hematoxylin and eosin. **(A)** ''Acute'' infarcts were defined as eosinophilic areas of coagulative necrosis without significant reactive cellular infiltrates, reflecting relatively recent acute or subacute necrosis. **(B)** ''Chronic'' infarcts were somewhat less clearly delineated and comprised infiltrates of mononuclear cells (lymphocytes and macrophages) along with variable degrees of fibroplasia and fibrosis. **(C)** Areas of acute and chronic hepatic necrosis were measured, combined, and averaged for each liver. Each box plot represents the minimum box plot represent the minimum, first quartile, median, third quartile, and maximum. *$p = 0.039$ for DMF *versus* vehicle. **(D)** Hepatic mRNA levels of proinflammatory cytokines IL-6, IL-1β, and IL-18 are expressed relative to 18S rRNA. *$p < 0.05$ for DMF *versus* vehicle. To see this illustration in color, the reader is referred to the web version of this article at www.liebertpub.com/ars

Table 3. Hematologic Parameters in Dimethyl Fumarate and Vehicle-Treated HbSS-Townes Mice

	Duration			
	1 week		*24 weeks*	
	Treatment			
	Vehicle	*DMF*	*Vehicle*	*DMF*
Age (weeks)	10	10	28	28
F-Cells	n.d.	n.d.	4.2 ± 1.3	8.8 ± 3.3[a]
Hematocrit (%)	35.3 ± 3.8	34.8 ± 2.2	23.5 ± 2.6[b]	22.0 ± 1.7[b]
Reticulocytes (%)	37.2 ± 6.0	41.0 ± 4.0	57.6 ± 11.2[b]	65.4 ± 11.5[b]
Irregular shaped RBC (%)	n.d.	n.d.	25.3 ± 0.5	19.0 ± 1.4[a]
Total plasma heme (μM)	46.6 ± 15.4	46.8 ± 13.2	39.0 ± 15.4	40.8 ± 12.0
Plasma hemoglobin (g/L)	$0.14 \pm .09$	0.28 ± 0.17	0.24 ± 0.14	$0.17 \pm .06$
Plasma LDH (mU/ml)	170 ± 7	170 ± 25	156 ± 21	135 ± 36
Spleen (% body weight)	n.d.	n.d.	6.8 ± 1.1	7.2 ± 1.0
White counts (cells/μl $\times 10^{-3}$)	32.7 ± 14.7	32.1 ± 13.3	24.9 ± 6.8	28.9 ± 10.4

HbSS-Townes mice were administered DMF (30 mg/kg/day; $n = 4$ mice) or vehicle (0.08% methyl cellulose; $n = 4$ mice) in drinking water for 24 weeks beginning at 4 weeks of age. Erythrocytes containing fetal hemoglobin (F-cells) were stained on blood smears by the Kleihauer–Betke method. Markers of hemolysis were measured, including packed RBC volume (hematocrit), reticulocytes, and spleen weight as a percentage of body weight. Values are mean ± SD.

[a] $p < 0.05$, vehicle *versus* DMF

[b] $p < 0.05$ 10 weeks *versus* 28 weeks of age.

LDH, lactate dehydrogenase; n.d., not determined; RBC, red blood cells.

haptoglobin, heme, or hemopexin. One possible explanation for unchanged plasma hemoglobin and heme levels despite increased haptoglobin and hemopexin is that the net input (hemolysis) and output (clearance) of plasma hemoglobin and heme were unchanged in DMF-treated sickle mice. The increased levels of plasma haptoglobin and hemopexin may provide a sink or vehicle to deliver plasma hemoglobin and heme safely to macrophages and the liver for degradation without activating the vessel wall (5, 39, 60, 61) and without necessarily increasing the plasma clearance rate. In contrast, when haptoglobin and hemopexin are depleted, hemoglobin and heme are more oxidatively reactive and able to promote proinflammatory responses in the vessel wall. Thus, the plasma heme that was circulating in DMF-treated sickle mice may have been rendered less reactive with the vessel wall, but without faster clearance rates. However, another possible interpretation is that plasma heme is irrelevant to the cytoprotection afforded by DMF. This latter interpretation seems unlikely, given the number of studies that have shown that HO-1 overexpression and heme degradation products, carbon monoxide and biliverdin, are cytoprotective in SCD and other inflammatory conditions.

Limiting hemolysis and the release of hemoglobin and heme into the vasculature is beneficial in SCD (45). Hydroxyurea, the only drug approved to date for treating SCD, works, in part, by inducing γ-globin and HbF expression, which replaces β^S-globin and HbS in erythrocytes, thereby inhibiting hemolysis (53). HbSS-Townes mice were created by knocking in human α and $^A\gamma\beta^S$ globins and thus are genetically capable of expressing human $^A\gamma$-globin and HbF. MMF, the primary metabolite of DMF, can induce γ-globin and HbF production in cultured human erythroid cells (46). In addition, Nrf2 can activate HbF production in human hematopoietic cells (38). Thus, chronic treatment of HbSS-Townes mice with DMF has the potential to improve hematological parameters by increasing circulating F-cells and limiting hemolysis. A chronic dosing study was carried out to evaluate long-term effects of DMF in improving disease parameters and anemia in HbSS-Townes mice. Administration of DMF in drinking water to HbSS-Townes mice for 24 weeks (~ 30 mg/kg/day) increased F-cells to 8.8% compared to 4.2% in vehicle-treated mice ($p = 0.043$), but did not alter hematocrits, reticulocyte counts, plasma LDH, or spleen weights, indicating that (i) the level of F-cells attained was not sufficient to significantly inhibit hemolysis as was recently described (53) and (ii) the anti-inflammatory effects of DMF were not attributable to a decrease in hemolysis. Furthermore, NY1DD mice do not have a γ-globin gene and do not express HbF; thus, the anti-inflammatory effects of DMF in NY1DD sickle mice cannot be attributed to induction of F-cells. The effect of DMF on F-cells, hemolysis, inflammation, and vaso-occlusive crises in human SCD patients has yet to be determined. It is possible that higher doses of DMF or other Nrf2 activating agents may achieve the desired levels of circulating F-cells in SCD.

While the protein(s) responsible for the cytoprotective effects of DMF on vaso-occlusion and hepatic necrosis in SCD mice cannot be precisely determined, these effects of DMF in sickle mice are likely attributable to induction of HO-1 and other Nrf2-responsive genes. Definitive studies directly linking the protective effects of DMF in SCD mice to Nrf2 activation and HO-1 activity would require DMF administration to Nrf2 and HO-1-deficient sickle mice. It has previously been demonstrated that DMF loses its cytoprotective effects on the nervous system when administered to Nrf2-deficient mice, thus proving the functional relevance of Nrf2 for the neuroprotective mechanism of action (36). Recently, investigators in Japan reported Nrf2 activation by ablation of its negative regulator, Keap1, which significantly inhibited inflammatory cytokines and adhesion molecule expression in SCD mice and reduced hepatic necrosis without inhibiting hemolysis or prolonging the life span of sickle RBC (31). However, the same

investigators reported a modest decrease in plasma heme levels in Keap1 ablated sickle mice, which were not seen in our studies. The reason for this difference is unclear, but could potentially be related to the dissimilar methods used for Nrf2 activation.

We propose that DMF may be an effective agent to prevent sickle crises through induction of HO-1, haptoglobin, hemopexin, FHC, and other anti-inflammatory proteins leading to inhibition of vaso-occlusion. These data combined with the modest induction of F-cells in SCD mice make DMF an ideal candidate for clinical trials in SCD patients.

Materials and Methods

Mice

All animal experiments were approved by the University of Minnesota's Institutional Animal Care and Use Committee. These studies utilized male and female NY1DD (17) and HbSS-Townes (65) transgenic sickle mice, age 8–14 weeks, with weights between 20 and 30 g, housed in SPF cages on a 12-h light/12-h dark cycle at 21°C. Chronic DMF dosing studies used HbSS-Townes mice beginning DMF or vehicle treatments at 4 weeks of age until 28 weeks of age. All animals were monitored daily, including weekends and holidays for health problems, food and water levels, and cage conditions. The NY1DD and HbSS-Townes mice are on C57BL/6 and mixed genetic backgrounds, respectively. The NY1DD mice are homozygous for deletion of the mouse β^{major} globin and express a human α and β^S globin transgene. The NY1DD mouse does not have a human γ-globin transgene. NY1DD mice have no anemia and a RBC half-life of 7 days (unpublished data). The HbSS-Townes mice were created by knocking in human α and $^A\gamma\beta^S$ globins into the sites where murine α and β globins were knocked out. HbSS-Townes mice have severe anemia and an RBC half-life of 2.5 days (7).

Oral DMF administration

The DMF used for these studies was purchased from Alfa Aesar, (cat no. A10402) or was a generous gift from Biogen. The vehicle (0.08% methyl cellulose) was obtained from Sigma-Aldrich (cat no. M7027). The vehicle was warmed to 37°C before dissolving the DMF at a final concentration of 1.5 mg/ml. NY1DD mice were gavaged with DMF (15 mg/kg body weight twice daily) or vehicle for 3 or 7 days as indicated. In chronic studies, DMF (0.15 mg/ml) or vehicle (0.08% methyl cellulose) was placed in the animals' drinking water for 24

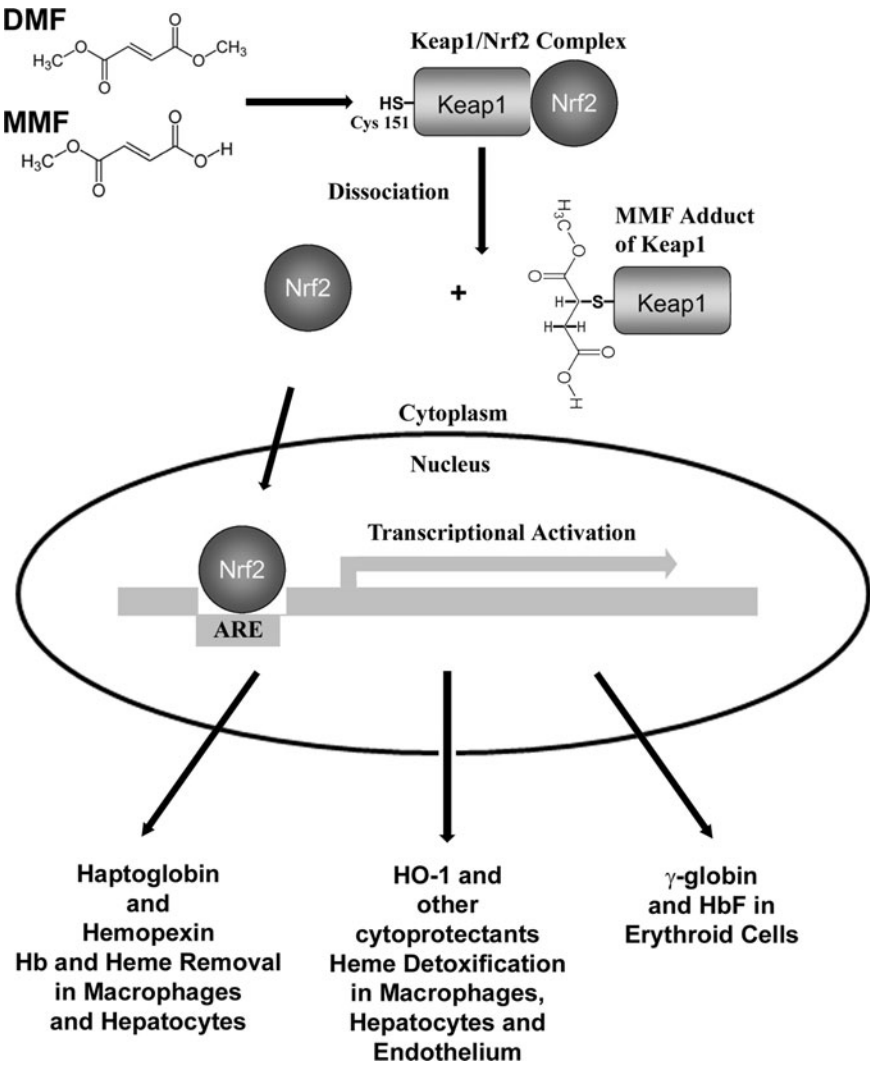

FIG. 8. Proposed model of heme detoxification and clearance by DMF in sickle cell disease. DMF and its primary intestinal metabolite MMF can both react with cysteine-151 on Keap1/Nrf2 complexes in the cytoplasm (53). The most probable reaction is a Michael addition of the nucleophilic sulfhydryl on Cys151 to the electrophilic alkene bond of MMF (20). Alkylation of the Keap1 sulfhydryl allows Nrf2 to dissociate from Keap1. Nrf2 then accumulates in the nucleus where it binds other transcription factors and ARE located in the regulatory regions of a battery of cellular defense genes and thereby activates transcription of those genes. Among the proteins induced are HO-1, FHC, and other cytoprotectants that can detoxify heme and haptoglobin and hemopexin that can bind hemoglobin and heme in the plasma and transport them safely to hepatocytes and macrophages for processing and degradation. In addition, γ-globin genes are expressed in hematopoietic cells, allowing the formation of HbF in RBC. ARE, antioxidant response elements; HbF, hemoglobin F; Keap1, kelch-like ECH-associated protein 1; MMF, monomethyl fumarate; RBC, red blood cells.

weeks as indicated. Providing DMF in drinking water for the chronic studies was likely less stressful than gavage. Fluid consumption was measured twice weekly. Mice drank the same volume of DMF and vehicle as mice given plain drinking water (~5 ml/day). This dose in drinking water (0.75 mg/day) in an average mouse weighing 0.025 kg is equivalent to the same dose administered to NY1DD mice by gavage (30 mg/kg). This dose (30 mg/kg) in mice is equivalent to a dose of 2.4 mg/kg in human adults using the body surface area normalization method (47). This is equivalent to the recommended starting dose of Tecfidera (120 mg twice a day) for multiple sclerosis patients. Regardless of the method or period of administration, DMF and vehicle appeared to be well tolerated; none of the mice administered DMF experienced any adverse events or death during treatment.

Measurement of vaso-occlusion (stasis)

Sickle mice were implanted with DSFCs as previously described (29). Three days later, mice with DSFCs were anesthetized with a mixture of ketamine (106 mg/kg) and xylazine (7.2 mg/kg), placed on a special intravital microscopy stage, and 20–30 flowing subcutaneous venules in the DSFC window were selected and mapped. After venule selection and mapping, hemin chloride (0.267 m*M*; Frontier Scientific), dissolved in sterile saline containing sodium carbonate (1.14 m*M*; Sigma-Aldrich) and D-sorbitol (0.96 m*M*; Sigma-Aldrich), was filtered (0.2 μm) and infused into the tail veins of mice (0.012 ml/kg, 3.2 μmol heme/kg body weight). All of the selected venules were reexamined at 1 and 4 h after hemin infusion, and the number of static (no flow) venules was counted and expressed as percent stasis. After the 4 h stasis measurement, mice were euthanized in a CO_2 atmosphere and the liver and kidneys were removed, flash frozen, and stored at −85°C. In one stasis experiment in DMF-treated NY1DD mice, HO-1 activity was inhibited by administration of SnPP (40 μmol/kg, i.p.) for 3 consecutive days with the third SnPP dose given 1 h before hemin infusion.

Quantitative RT-PCR

Total RNA was extracted from tissues (~30 mg) using RNeasy Mini kit (Qiagen). RNA was digested with RNase-free DNase I (Roche) to remove any contaminating DNA, and the DNase I was heat-inactivated by incubation at 75°C for 10 min. cDNA was generated from 500 ng RNA using qScript cDNA Supermix (Quanta BioSciences). qPCR was performed in triplicate once or twice on a LightCycler 480 (Roche) using FastStart Universal SYBR Green Master (Roche). Primer sequences used are provided in Supplementary Table S1.

Isolation of organ subcellular fractions and Western blots

Microsomes and nuclear extracts were isolated as described (9) from the livers and kidneys of DMF- and vehicle-treated mice. Cytosolic supernatants were collected after pelleting of liver microsomes at 105,000 *g*. The protein concentrations of organ subcellular fractions were measured with a Bradford dye-binding assay (Bio-Rad), and 30 μg of protein from the indicated fractions was run on SDS-PAGE for Western blots. Blots of subcellular fractions were immunostained with primary antibodies to Nrf2 (Cell Signaling no. 8882), GSTA2 (Abcam no. ab135709), HO-1 (Enzo no. ADI-OSA-111), FHC (Origene no. TA301280), haptoglobin (Abcam no. 135835 or Proteintech no. 16665-1-AP), hemopexin (BioVision no. 3899-200), phospho (Ser536, Cell Signaling no. 3031) and total (Cell Signaling no. 3034) NF-κB p65, VCAM-1 (Abcam no. ab174279), ICAM-1 (Abcam no. ab124759), E-selectin (BioVision, no. 3631), and TLR4 (Antibodies-online no. ABIN361724). Bound primary antibodies were labeled with goat anti-rabbit secondary antibodies conjugated to alkaline phosphatase (Santa Cruz no. SC-2007) and visualized with ECF™ substrate (GE Healthcare) and a Storm™ Reader (GE Healthcare). Blots were stripped with Restore Stripping Buffer (Thermo Scientific) and reprobed with rabbit anti-GAPDH (Sigma-Aldrich no. G9545) as a loading control.

Plasma samples were run on SDS-PAGE for Western blots using 1 μl of each plasma sample per lane. The blot was immunostained for mouse haptoglobin (R&D Systems no. AF4409) or hemopexin (R&D Systems no. MAB7007). The primary antibodies were visualized with donkey anti-sheep or goat anti-rat IgG conjugated to alkaline phosphatase (Santa Cruz no. SC-2474 or no. SC-2021). Blots were visualized with ECF substrate, stripped as described above, and reprobed with goat anti-mouse IgG conjugated to alkaline phosphatase (Santa Cruz no. SC-2008) as a loading control. Immunoreactive bands on images were quantitated using ImageJ software (NIH). Enrichment of bands was measured by calculating the ratios of DMF to vehicle band intensities.

Histology and histomorphometry

Livers were fixed in 10% neutral buffered formalin. Formalin-fixed livers were cut into several 2–3 mm thick sections, processed through a series of alcohols of increasing concentration and xylene, embedded in paraffin, and 4 μm thick sections were cut and stained with hematoxylin and eosin. For quantification of hepatic infarcts and necrosis, digital images of liver were taken with a Spot Insight 4 MP CCD Scientific Color Digital camera (Diagnostic Instruments) mounted on a Nikon E-800 microscope. ''Acute'' and ''chronic'' infarcts were delineated and their areas measured using Image-Pro Plus version 6.2 (Media Cybernetics). Acute infarcts were defined as eosinophilic areas of coagulative necrosis without significant reactive cellular infiltrates, reflecting relatively recent acute or subacute necrosis. Chronic infarcts were somewhat less clearly delineated and comprised infiltrates of mononuclear cells (lymphocytes and macrophages) along with variable degrees of fibroplasia and fibrosis; these lesions were interpreted to represent various stages of removal and repair of the regions of acute infarction. Areas of acute and chronic necrosis were combined for analysis.

Blood collection

Blood was collected for measurement of F-cells, hematocrits, reticulocytes, and plasma haptoglobin and hemopexin. NY1DD and HbSS-Townes mice without DSFCs were administered DMF or vehicle in their drinking water for indicated times. At the end of treatment, mice were anesthetized with a mixture of urethane (1 g/kg) and alpha-chloralose (100 mg/kg). Heparinized blood was collected from the abdominal aorta and placed on ice before processing. Plasma was isolated by centrifugation and frozen at −85°C.

Plasma hemoglobin and heme

Plasma hemoglobin was measured spectrophotometrically by the Fairbanks AII method (18). Total plasma heme levels were measured colorimetrically at 400 nm using a QuantiChrom™ Heme Assay Kit (BioAssay Systems). This method measures total plasma heme, including heme bound to microparticles, hemoglobin, albumin, haptoglobin, and hemopexin (unpublished data). In some experiments, we used the same heme assay to measure heme in plasma that was subjected to a second spin through a Microcon YM-3 column (EMD Millipore) at 20,000 *g* at 4°C, for 2 h to prepare a protein-depleted plasma fraction devoid of molecules of MW >3 kDa as previously described (22).

F-cells

Heparinized whole blood was collected from the abdominal aorta of male and female HbSS-Townes mice administered DMF ($\sim$30 mg/kg/day; $n=4$ mice) or vehicle (0.08% methyl cellulose; $n=4$ mice) in drinking water for 24 weeks beginning at 4 weeks of age. F-cells were stained on blood smears by the Kleihauer–Betke method (32) using a fetal cell stain kit (Simmler) according to the manufacturer's instructions. F-cells and total erythrocytes were counted in 4 separate microscopic fields at 100× magnification for each mouse. The F-cells were expressed as a percentage of total erythrocytes. Human fetal cord blood was used as a positive control.

Hematocrits

Percent packed RBC (% hematocrits) were measured in capillary tubes using the same heparinized blood described above using a microcapillary reader (IEC) after centrifugation in a microcapillary centrifuge (IEC).

Reticulocytes

Reticulocytes were measured using the same heparinized blood described above. Blood smears were stained with methylene blue. Reticulocytes, identified by their DNA staining, and total erythrocytes were counted in four separate microscopic fields for each mouse. Reticulocytes were expressed as a percentage of total erythrocytes.

Irregular shaped RBC

Blood smears from HbSS-Townes mice were stained with Wright's stain, and three representative fields per slide were photographed under a microscope at 100× magnification. Irregular and normal shaped RBC were counted (mean = 99 $\pm$15 cells/slide) and the irregular shaped RBC were expressed as a percentage of total RBC. The irregular shaped RBC included teardrop, schistocyte, elliptocyte, bite, and sickle cells (37).

Plasma LDH and AST

Plasma LDH and AST enzyme activities were measured in plasma from HbSS-Townes mice after 24 weeks of treatment with DMF or vehicle using kits from Sigma-Aldrich.

Urine creatinine

Twenty-four-hour urine samples were collected from HbSS-Townes mice after 22 weeks of treatment with DMF or vehicle in drinking water. Mice had access to the DMF or vehicle drinking water during the 24-h collection period. Creatinine was measured in urine samples using a kit from BioAssay Systems.

Markers of oxidative stress

Protein carbonyls and 4-HNE were measured in liver subfractions, and 8-hydroxydeoxyguanosine was measured in 24-h urine samples.

White counts

The total white blood cell counts were counted manually using a hemocytometer.

Statistics

Analyses were performed with SigmaStat 3.5 for Windows (Systat Software). Comparisons of multiple treatment groups were made using one-way analysis of variance (ANOVA) (Holm-Sidak method). For comparing two groups, an unpaired *t*-test was used for groups with normal distributions and a Mann–Whitney rank sum test was used for groups that failed the normality test.

Acknowledgments

This work was supported by grants from NHLBI (R01 HL114567-05 to G.M.V. and J.D.B. and Biogen to J.D.B. and G.M.V.). The authors would like to thank Josh Parker for quantitative image analysis of liver necrosis.

Author Disclosure Statement

Some of the research funding to J.D.B. and G.M.V. came from Biogen, which owns the rights to Tecfidera. For all other authors, no competing financial interests exist.

References

1. Albrecht P, Bouchachia I, Goebels N, Henke N, Hofstetter HH, Issberner A, Kovacs Z, Lewerenz J, Lisak D, Maher P, Mausberg AK, Quasthoff K, Zimmermann C, Hartung HP, and Methner A. Effects of dimethyl fumarate on neuroprotection and immunomodulation. *J Neuroinflammation* 9: 163, 2012.
2. Balla G, Vercellotti GM, Muller-Eberhard U, Eaton J, and Jacob HS. Exposure of endothelial cells to free heme potentiates damage mediated by granulocytes and toxic oxygen species. *Lab Invest* 64: 648–655, 1991.
3. Barnard ML, Muller-Eberhard U, and Turrens JF. Protective role of hemopexin on heme-dependent lung oxidative stress. *Biochem Biophys Res Commun* 192: 82–87, 1993.
4. Bean CJ, Boulet SL, Ellingsen D, Pyle ME, Barron-Casella EA, Casella JF, Payne AB, Driggers J, Trau HA, Yang G, Jones K, Ofori-Acquah SF, Hooper WC, and DeBaun MR. Heme oxygenase-1 gene promoter polymorphism is associated with reduced incidence of acute chest syndrome among children with sickle cell disease. *Blood* 120: 3822–3828, 2012.
5. Belcher JD, Chen C, Nguyen J, Milbauer L, Abdulla F, Alayash AI, Smith A, Nath KA, Hebbel RP, and Vercellotti GM. Heme triggers TLR4 signaling leading to endothelial cell activation and vaso-occlusion in murine sickle cell disease. *Blood* 123: 377–390, 2014.

6. Belcher JD, Mahaseth H, Welch TE, Otterbein LE, Hebbel RP, and Vercellotti GM. Heme oxygenase-1 is a modulator of inflammation and vaso-occlusion in transgenic sickle mice. *J Clin Invest* 116: 808–816, 2006.
7. Belcher JD, Nath KA, and Vercellotti GM. Vasculotoxic and pro-inflammatory effects of plasma heme: cell signaling and cytoprotective responses. *ISRN Oxid Med* 2013: Article ID 831596, 2013.
8. Belcher JD, Nguyen J, Chen C, Abdulla F, Nguyen P, Nguyen M, Zhang P, Xu P, Slipek NJ, and Vercellotti, GM. Dimethyl fumarate induces cytoprotection and inhibits vaso-occlusion in transgenic sickle mice. *Am Soc Hematol* 124: 219, 2014.
9. Belcher JD, Vineyard JV, Bruzzone CM, Chen C, Beckman JD, Nguyen J, Steer CJ, and Vercellotti GM. Heme oxygenase-1 gene delivery by Sleeping Beauty inhibits vascular stasis in a murine model of sickle cell disease. *J Mol Med (Berl)* 88: 665–675, 2010.
10. Belcher JD, Young M, Chen C, Nguyen J, Burhop K, Tran P, and Vercellotti GM. MP4CO, a pegylated hemoglobin saturated with carbon monoxide, is a modulator of HO-1, inflammation, and vaso-occlusion in transgenic sickle mice. *Blood* 122: 2757–2764, 2013.
11. Boretti FS, Buehler PW, D'Agnillo F, Kluge K, Glaus T, Butt OI, Jia Y, Goede J, Pereira CP, Maggiorini M, Schoedon G, Alayash AI, and Schaer DJ. Sequestration of extracellular hemoglobin within a haptoglobin complex decreases its hypertensive and oxidative effects in dogs and guinea pigs. *J Clin Invest* 119: 2271–2280, 2009.
12. Boyle JJ, Johns M, Lo J, Chiodini A, Ambrose N, Evans PC, Mason JC, and Haskard DO. Heme induces heme oxygenase 1 via Nrf2: role in the homeostatic macrophage response to intraplaque hemorrhage. *Arterioscler Thromb Vasc Biol* 31: 2685–2691, 2011.
13. Camus SM, De Moraes JA, Bonnin P, Abbyad P, Le Jeune S, Lionnet F, Loufrani L, Grimaud L, Lambry JC, Charue D, Kiger L, Renard JM, Larroque C, Le Clesiau H, Tedgui A, Bruneval P, Barja-Fidalgo C, Alexandrou A, Tharaux PL, Boulanger CM, and Blanc-Brude OP. Circulating cell membrane microparticles transfer heme to endothelial cells and trigger vasoocclusions in sickle cell disease. *Blood* 125: 3805–3814, 2015.
14. Chorley BN, Campbell MR, Wang X, Karaca M, Sambandan D, Bangura F, Xue P, Pi J, Kleeberger SR, and Bell DA. Identification of novel NRF2-regulated genes by ChIP-Seq: influence on retinoid X receptor alpha. *Nucleic Acids Res* 40: 7416–7429, 2012.
15. Duffy S, So A, and Murphy TH. Activation of endogenous antioxidant defenses in neuronal cells prevents free radical-mediated damage. *J Neurochem* 71: 69–77, 1998.
16. Durand RE and Olive PL. Flow cytometry techniques for studying cellular thiols. *Radiat Res* 95: 456–470, 1983.
17. Fabry ME, Nagel RL, Pachnis A, Suzuka SM, and Costantini F. High expression of human beta S- and alpha-globins in transgenic mice: hemoglobin composition and hematological consequences. *Proc Natl Acad Sci U S A* 89: 12150–12154, 1992.
18. Fairbanks VF, Ziesmer SC, and O'Brien PC. Methods for measuring plasma hemoglobin in micromolar concentration compared. *Clin Chem* 38: 132–140, 1992.
19. Fang J, Qin H, Seki T, Nakamura H, Tsukigawa K, Shin T, and Maeda H. Therapeutic potential of pegylated hemin for reactive oxygen species-related diseases via induction of heme oxygenase-1: results from a rat hepatic ischemia/reperfusion injury model. *J Pharmacol Exp Ther* 339: 779–789, 2011.
20. Foresti R, Bains SK, Pitchumony TS, de Castro Bras LE, Drago F, Dubois-Rande JL, Bucolo C, and Motterlini R. Small molecule activators of the Nrf2-HO-1 antioxidant axis modulate heme metabolism and inflammation in BV2 microglia cells. *Pharmacol Res* 76: 132–148, 2013.
21. Frycak P, Zdrahal Z, Ulrichova J, Wiegrebe W, and Lemr K. Evidence of covalent interaction of fumaric acid esters with sulfhydryl groups in peptides. *J Mass Spectrom* 40: 1309–1318, 2005.
22. Ghosh S, Adisa OA, Chappa P, Tan F, Jackson KA, Archer DR, and Ofori-Acquah SF. Extracellular hemin crisis triggers acute chest syndrome in sickle mice. *J Clin Invest* 123: 4809–4820, 2013.
23. Gold R, Kappos L, Arnold DL, Bar-Or A, Giovannoni G, Selmaj K, Tornatore C, Sweetser MT, Yang M, Sheikh SI, and Dawson KT. Placebo-controlled phase 3 study of oral BG-12 for relapsing multiple sclerosis. *N Engl J Med* 367: 1098–1107, 2012.
24. Held KD, Epp ER, Clark EP, and Biaglow JE. Effect of dimethyl fumarate on the radiation sensitivity of mammalian cells in vitro. *Radiat Res* 115: 495–502, 1988.
25. Hunt RC, Hunt DM, Gaur N, and Smith A. Hemopexin in the human retina: protection of the retina against heme-mediated toxicity. *J Cell Physiol* 168: 71–80, 1996.
26. Hvidberg V, Maniecki MB, Jacobsen C, Hojrup P, Moller HJ, and Moestrup SK. Identification of the receptor scavenging hemopexin-heme complexes. *Blood* 106: 2572–2579, 2005.
27. Ishii T, Itoh K, Takahashi S, Sato H, Yanagawa T, Katoh Y, Bannai S, and Yamamoto M. Transcription factor Nrf2 coordinately regulates a group of oxidative stress-inducible genes in macrophages. *J Biol Chem* 275: 16023–16029, 2000.
28. Jison ML, Munson PJ, Barb JJ, Suffredini AF, Talwar S, Logun C, Raghavachari N, Beigel JH, Shelhamer JH, Danner RL, and Gladwin MT. Blood mononuclear cell gene expression profiles characterize the oxidant, hemolytic, and inflammatory stress of sickle cell disease. *Blood* 104: 270–280, 2004.
29. Kalambur VS, Mahaseth H, Bischof JC, Kielbik MC, Welch TE, Vilback A, Swanlund DJ, Hebbel RP, Belcher JD, and Vercellotti GM. Microvascular blood flow and stasis in transgenic sickle mice: utility of a dorsal skin fold chamber for intravital microscopy. *Am J Hematol* 77: 117–125, 2004.
30. Kato GJ. Haptoglobin halts hemoglobin's havoc. *J Clin Invest* 119: 2140–2142, 2009.
31. Keleku-Lukwete N, Suzuki M, Otsuki A, Tsuchida K, Katayama S, Hayashi M, Naganuma E, Moriguchi T, Tanabe O, Engel JD, Imaizumi M, and Yamamoto M. Amelioration of inflammation and tissue damage in sickle cell model mice by Nrf2 activation. *Proc Natl Acad Sci U S A* 112: 12169–12174, 2015.
32. Kleihauer E, Braun H, and Betke K. [Demonstration of fetal hemoglobin in erythrocytes of a blood smear]. *Klin Wochenschr* 35: 637–638, 1957.
33. Lanaro C, Franco-Penteado CF, Albuqueque DM, Saad ST, Conran N, and Costa FF. Altered levels of cytokines and inflammatory mediators in plasma and leukocytes of sickle cell anemia patients and effects of hydroxyurea therapy. *J Leukoc Biol* 85: 235–242, 2009.

34. Li RC, Saleem S, Zhen G, Cao W, Zhuang H, Lee J, Smith A, Altruda F, Tolosano E, and Dore S. Heme-hemopexin complex attenuates neuronal cell death and stroke damage. *J Cereb Blood Flow Metab* 29: 953–964, 2009.
35. Lin SX, Lisi L, Dello Russo C, Polak PE, Sharp A, Weinberg G, Kalinin S, and Feinstein DL. The anti-inflammatory effects of dimethyl fumarate in astrocytes involve glutathione and haem oxygenase-1. *ASN Neuro* 3: pii: e00055, 2011.
36. Linker RA, Lee DH, Ryan S, van Dam AM, Conrad R, Bista P, Zeng W, Hronowsky X, Buko A, Chollate S, Ellrichmann G, Bruck W, Dawson K, Goelz S, Wiese S, Scannevin RH, Lukashev M, and Gold R. Fumaric acid esters exert neuroprotective effects in neuroinflammation via activation of the Nrf2 antioxidant pathway. *Brain* 134: 678–692, 2011.
37. Lynch EC. Peripheral blood smear. In: *Clinical Methods: The History, Physical, and Laboratory Examinations*, edited by Walker HK, Hall WD, and Hurst JW. Boston: Butterworths, 1990, pp. 732–734.
38. Macari ER and Lowrey CH. Induction of human fetal hemoglobin via the NRF2 antioxidant response signaling pathway. *Blood* 117: 5987–5997, 2011.
39. Mollan TL, Jia Y, Banerjee S, Wu G, Kreulen RT, Tsai AL, Olson JS, Crumbliss AL, and Alayash AI. Redox properties of human hemoglobin in complex with fractionated dimeric and polymeric human haptoglobin. *Free Radic Biol Med* 69: 265–277, 2014.
40. Muller-Eberhard U. [47] Hemopexin. In: *Methods in Enzymology*, edited by DiSabato G. Academic Press: Orlando, Florida, 1988, pp. 536–565.
41. Muller-Eberhard U, Javid J, Liem HH, Hanstein A, and Hanna M. Plasma concentrations of hemopexin, haptoglobin and heme in patients with various hemolytic diseases. *Blood* 32: 811–815, 1968.
42. Murphy TH, Yu J, Ng R, Johnson DA, Shen H, Honey CR, and Johnson JA. Preferential expression of antioxidant response element mediated gene expression in astrocytes. *J Neurochem* 76: 1670–1678, 2001.
43. Nath KA, Grande JP, Haggard JJ, Croatt AJ, Katusic ZS, Solovey A, and Hebbel RP. Oxidative stress and induction of heme oxygenase-1 in the kidney in sickle cell disease. *Am J Pathol* 158: 893–903, 2001.
44. Niture SK, Khatri R, and Jaiswal AK. Regulation of Nrf2-an update. *Free Radic Biol Med* 66: 36–44, 2014.
45. Nouraie M, Lee JS, Zhang Y, Kanias T, Zhao X, Xiong Z, Oriss TB, Zeng Q, Kato GJ, Gibbs JS, Hildesheim ME, Sachdev V, Barst RJ, Machado RF, Hassell KL, Little JA, Schraufnagel DE, Krishnamurti L, Novelli E, Girgis RE, Morris CR, Rosenzweig EB, Badesch DB, Lanzkron S, Castro OL, Goldsmith JC, Gordeuk VR, and Gladwin MT. The relationship between the severity of hemolysis, clinical manifestations and risk of death in 415 patients with sickle cell anemia in the US and Europe. *Haematologica* 98: 464–472, 2013.
46. Promsote W, Makala L, Li B, Smith SB, Singh N, Ganapathy V, Pace BS, and Martin PM. Monomethylfumarate induces gamma-globin expression and fetal hemoglobin production in cultured human retinal pigment epithelial (RPE) and erythroid cells, and in intact retina. *Invest Ophthalmol Vis Sci* 55: 5382–5393, 2014.
47. Reagan-Shaw S, Nihal M, and Ahmad N. Dose translation from animal to human studies revisited. *FASEB J* 22: 659–661, 2008.
48. Scannevin RH, Chollate S, Jung MY, Shackett M, Patel H, Bista P, Zeng W, Ryan S, Yamamoto M, Lukashev M, and Rhodes KJ. Fumarates promote cytoprotection of central nervous system cells against oxidative stress via the nuclear factor (erythroid-derived 2)-like 2 pathway. *J Pharmacol Exp Ther* 341: 274–284, 2012.
49. Schaer DJ, Buehler PW, Alayash AI, Belcher JD, and Vercellotti GM. Hemolysis and free hemoglobin revisited: exploring hemoglobin and hemin scavengers as a novel class of therapeutic proteins. *Blood* 121: 1276–1284, 2013.
50. Shen G, Xu C, Hu R, Jain MR, Gopalkrishnan A, Nair S, Huang MT, Chan JY, and Kong AN. Modulation of nuclear factor E2-related factor 2-mediated gene expression in mice liver and small intestine by cancer chemopreventive agent curcumin. *Mol Cancer Ther* 5: 39–51, 2006.
51. Singh S, Vrishni S, Singh BK, Rahman I, and Kakkar P. Nrf2-ARE stress response mechanism: a control point in oxidative stress-mediated dysfunctions and chronic inflammatory diseases. *Free Radic Res* 44: 1267–1288, 2010.
52. Spencer SR, Wilczak CA, and Talalay P. Induction of glutathione transferases and NAD(P)H:quinone reductase by fumaric acid derivatives in rodent cells and tissues. *Cancer Res* 50: 7871–7875, 1990.
53. Steinberg MH, Chui DH, Dover GJ, Sebastiani P, and Alsultan A. Fetal hemoglobin in sickle cell anemia: a glass half full? *Blood* 123: 481–485, 2014.
54. Takaya K, Suzuki T, Motohashi H, Onodera K, Satomi S, Kensler TW, and Yamamoto M. Validation of the multiple sensor mechanism of the Keap1-Nrf2 system. *Free Radic Biol Med* 53: 817–827, 2012.
55. Thimmulappa RK, Mai KH, Srisuma S, Kensler TW, Yamamoto M, and Biswal S. Identification of Nrf2-regulated genes induced by the chemopreventive agent sulforaphane by oligonucleotide microarray. *Cancer Res* 62: 5196–5203, 2002.
56. Tolosano E, Fagoonee S, Morello N, Vinchi F, and Fiorito V. Heme scavenging and the other facets of hemopexin. *Antioxid Redox Signal* 12: 305–320, 2010.
57. Tsuji Y, Ayaki H, Whitman SP, Morrow CS, Torti SV, and Torti FM. Coordinate transcriptional and translational regulation of ferritin in response to oxidative stress. *Mol Cell Biol* 20: 5818–5827, 2000.
58. Vercellotti GM, Khan FB, Nguyen J, Chen C, Bruzzone CM, Bechtel H, Brown G, Nath KA, Steer CJ, Hebbel RP, and Belcher JD. H-ferritin ferroxidase induces cytoprotective pathways and inhibits microvascular stasis in transgenic sickle mice. *Front Pharmacol* 5: 79, 2014.
59. Vercellotti GM, Zhang P, Chen C, Nguyen J, Abdulla F, Nguyen P, Nowotny C, Irfnullah A, Smith A, Steer CJ, and Belcher JD. Hemopexin gene therapy inhibits inflammation and vaso-occlusion in transgenic sickle cell mice. In: *American Society of Hematology Annual Meeting & Exposition*. Orlando, FL: ASH, 2015, p. 412.
60. Vinchi F, De Franceschi L, Ghigo A, Townes T, Cimino J, Silengo L, Hirsch E, Altruda F, and Tolosano E. Hemopexin therapy improves cardiovascular function by preventing heme-induced endothelial toxicity in mouse models of hemolytic diseases. *Circulation* 127: 1317–1329, 2013.
61. Vinchi F, Gastaldi S, Silengo L, Altruda F, and Tolosano E. Hemopexin prevents endothelial damage and liver congestion in a mouse model of heme overload. *Am J Pathol* 173: 289–299, 2008.
62. Walsh J, Jenkins RE, Wong M, Olayanju A, Powell H, Copple I, O'Neill PM, Goldring CE, Kitteringham NR, and Park BK. Identification and quantification of the basal and inducible Nrf2-dependent proteomes in mouse liver: bio-

chemical, pharmacological and toxicological implications. *J Proteomics* 108: 171–187, 2014.
63. Wang Y, Santa-Cruz K, DeCarli C, and Johnson JA. NAD(P)H:quinone oxidoreductase activity is increased in hippocampal pyramidal neurons of patients with Aalzheimer's disease. *Neurobiol Aging* 21: 525–531, 2000.
64. Wasserman WW and Fahl WE. Functional antioxidant responsive elements. *Proc Natl Acad Sci U S A* 94: 5361–5366, 1997.
65. Wu LC, Sun CW, Ryan TM, Pawlik KM, Ren J, and Townes TM. Correction of sickle cell disease by homologous recombination in embryonic stem cells. *Blood* 108: 1183–1188, 2006.

Address correspondence to:
Dr. John D. Belcher
Division of Hematology, Oncology and Transplantation
Department of Medicine
Vascular Biology Center
University of Minnesota
420 Delaware Street SE, MMC 480
Minneapolis, MN 55455

E-mail: belcher@umn.edu

Date of first submission to ARS Central, November 10, 2015; date of final revised submission, February 23, 2016; date of acceptance, February 24, 2016.

Abbreviations Used

4-HNE = 4-hydroxynonenal
ANOVA = analysis of variance
ARE = antioxidant response element
AST = aspartate aminotransferase
DMF = dimethyl fumarate
DSFC = dorsal skinfold chamber
F-cells = hemoglobin F-containing red blood cells
FHC = ferritin heavy chain
GSTA2 = glutathione S-transferase alpha 2
HbF = hemoglobin F
HbS = hemoglobin S
HO-1 = heme oxygenase-1
ICAM-1 = intercellular adhesion molecule-1
Keap1 = kelch-like ECH-associated protein 1
LDH = lactate dehydrogenase
LRP1/CD91 = low-density lipoprotein receptor-related protein 1
MMF = monomethyl fumarate
NF-κB = nuclear factor-kappa B
Nrf2 = nuclear factor erythroid-2-related factor-2
RBC = red blood cells
SCD = sickle cell disease
SnPP = tin protoporphyrin
TLR4 = toll-like receptor 4
VCAM-1 = vascular cell adhesion molecule-1